ACS Sustainable Chemistry & Engineering

Letter

pubs.acs.org/journal/ascecg

A Facile Method for Generating Designer Block Copolymers from Functionalized Lignin Model Compounds

Angela L. Holmberg,[†,∥] Joseph F. Stanzione, III,[†,‡,§,∥] Richard P. Wool,*[,†,‡] and Thomas H. Epps, III*[,†]

[†]Department of Chemical and Biomolecular Engineering, University of Delaware, Newark, Delaware 19716, United States

[‡]Center for Composite Materials, University of Delaware, Newark, Delaware 19716, United States

Supporting Information

ABSTRACT: We report a versatile scheme for the synthesis of renewable homopolymers and block copolymers (BCPs) via the functionalization and subsequent controlled reversible addition−fragmentation chain transfer (RAFT) polymerization of vanillin, a possible lignin derivative. The vanillin-based homopolymers exhibit glass transition temperatures (120 °C) and degradation temperatures (≥300 °C) comparable to polystyrene, indicating that these and similar polymers may serve as suitable alternatives to petroleum-based materials. Additionally, by employing controlled polymerization techniques, a vanillin-based homopolymer was chain-extended with lauryl methacrylate, a model fatty acid-derived monomer, to generate nanostructured BCPs. As one example, these elastomeric copolymers can self-assemble into a body-centered cubic array of vanillin-based nanospheres in a poly(lauryl methacrylate) matrix, which we demonstrated via small-angle X-ray scattering (SAXS) and transmission electron microscopy (TEM) analysis. This work provides a blueprint for the controlled polymerization of phenolic lignin model compounds and their subsequent chain extension with various biobased comonomers, enabling the de novo design and generation of new homopolymers and BCPs with tunable properties.

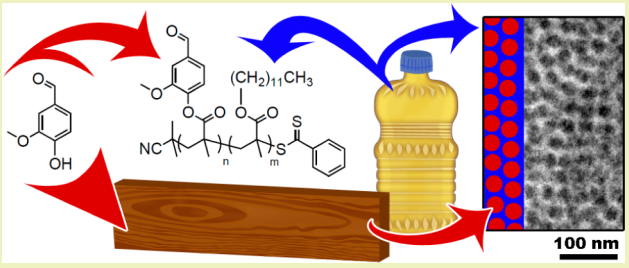

KEYWORDS: *Vanillin, Lignin, Renewable, Biobased, Block copolymer, RAFT, Self-assembly*

INTRODUCTION

Styrenic block copolymers (BCPs) are desirable for a number of areas, including adhesives, footwear, and asphalt,[1] but polystyrene (PS) blocks are derived from toxic nonrenewable monomers.[2] Hence, there is a critical need for designing sustainable PS-alternatives, not just for BCPs but also for plastics, foams, adhesives, and composite resins. For polymers to serve as suitable and sustainable PS-alternatives, they must have the potential to meet commodity production volumes without compromising food, water, or land supplies;[3] come from nontoxic and nonvolatile monomers;[4] accommodate BCP syntheses;[5] and exhibit properties comparable to PS, for which the most general properties relate to glass transition temperature ($T_g \approx 100$ °C), thermal degradation, and BCP nanoscale self-assembly. Numerous reasons suggest lignin, nature's most abundant aromatic polymer, as a leading candidate for sourcing sustainable PS-alternatives that meet the aforementioned requirements. Lignin is a renewable industrial waste harvested on a scale of ∼70 million tons/year from pulp and paper mills[6] and can be converted into numerous aromatic chemicals.[7−9] In this regard, lignin is more sustainable than other renewable BCP feedstocks, such as scarce tulips[10,11] and mint[12] or edible corn and sugars,[13] as it is neither rare nor a food source.[3] The diverse array of phenolic monomers with similar structure to styrene, including vanillin, guaiacols, catechols, cresols, and other phenolic lignin model compounds (LMCs) afforded by lignin pyrolysis,[7,8] supports the prospect of tunable properties to meet specific needs simply through monomer choice.[14] Herein, we establish a facile procedure for synthesizing homopolymers and BCPs almost entirely from renewable industrial waste with characteristics similar to styrene-containing polymers.

RESULTS AND DISCUSSION

A polymerizable LMC was derived from 4-hydroxy-3-methoxybenzaldehyde (vanillin, shown in Scheme 1), a chemical manufactured from lignin commercially on a scale of at least 17 000 ton/year.[15] Vanillin also is beneficial for its low toxicity suggested by its inclusion in foods and perfumes and its low volatility relative to carcinogenic styrene. For the BCP studies, a low-T_g comonomer possibly derived from fatty acids was selected to imitate the soft polyisoprene (PI) or polybutadiene (PB) blocks most commonly associated with PS. Fatty acids also exhibit benefits regarding low toxicity, low volatility, sustainable scale-up (∼150 million tons/year of fatty acids including industrial waste from used cooking oil[6]), and diversity in monomer structure and properties driven simply by monomer choice.[16−20] Promising applications for fatty acid-based BCPs include actuators,[21] engine oil lubricants,[22] thermoplastic elastomers,[5,23−25] and pressure-sensitive adhe-

Received: November 27, 2013
Revised: January 8, 2014
Published: January 21, 2014

 © 2014 American Chemical Society

Scheme 1. Synthesis of Biobased Polymers 2–4[a,b]

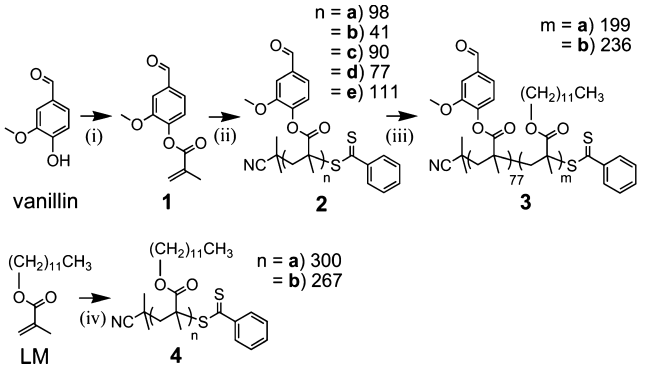

[a]Reagents and conditions: (i) methacrylic anhydride, 4-dimethylaminopyridine, 55 °C;[26] (ii) CTA, AIBN, 1,4-dioxane for **2a–d** or anisole for **2e**, 72 °C; (iii) LM, AIBN, 1,4-dioxane for **3a** or 1:3 v/v 2-butanone/anisole for **3b**, 72 °C; and (iv) CTA, AIBN, 1,4-dioxane, 72 °C. [b]Degrees of polymerization from SEC (n) or ^{1}H NMR composition (m).

sives.[5] The example comonomer in this work is lauryl methacrylate (LM, biobased content = 75%), a potential derivative of lauric acid.[16]

A methacrylate group was attached to vanillin such that it could be polymerized in a controlled manner. Conversion of vanillin to monomer **1** (4-methacryloyloxy-3-methoxybenzaldehyde or methacrylated vanillin, biobased content = 67%) was achieved via base-catalyzed esterification of the phenolic group with methacrylic anhydride [Scheme 1 (i)].[26] This chemistry was favored over acid-catalyzed esterification, Steglich esterification, and similar methods due to its solvent-free moderate-temperature conditions,[26] but optimization is needed in terms of reducing solvent consumption during monomer purification.

The biobased methacrylate monomers were polymerized by reversible addition–fragmentation chain transfer (RAFT), a reasonably green technique noted for its moderate temperatures and favorable atom economy, which includes minimal solvent volumes, tolerance to unprotected functional groups, low dispersities ($Đ = M_w/M_n$), and recyclable raw materials.[27] Scheme 1 (ii) and (iv) depict example RAFT homopolymerizations of vanillin-based **1** and fatty acid-based LM, respectively. 2,2′-Azobisisobutyronitrile (AIBN) served as the radical initiator, and 2-cyano-2-propyl benzodithioate served as the chain transfer agent (CTA). As represented in Scheme 1 (iii), the vanillin-based homopolymer **2d** ($M_{n,SEC}$ = 17,000 g/mol, $Đ$ = 1.34) served as the macro-CTA for biobased BCPs **3a** ($M_{n,SEC}$ = 56,000 g/mol, $Đ$ = 1.50, 20 vol % **2d**-block, biobased content = 73%) and **3b** ($M_{n,SEC}$ = 60,000 g/mol, $Đ$ = 1.38, 17 vol % **2d**-block, biobased content = 73%). E-factors for the homopolymerizations of vanillin- and fatty acid-based methacrylates were less than 400 and 100, respectively, and E-factors for the block copolymerizations, including the homopolymerization steps, were ~500. The E-factor estimates do not include monomer syntheses, as the fatty acid-based monomer was purchased. These values and the overall sustainability of the polymerizations could be improved by optimizing synthesis conditions, minimizing solvent consumption in the workup procedure, implementing greener solvents (e.g., anisole in place of 1,4-dioxane as with **2e**), and recycling the solvents and monomer. In each ^{1}H NMR spectrum of fully purified vanillin-based polymers **2b–e**, **3a**, and **3b**, the ratio of the aldehyde (Ar–C*H*O) to methoxy (Ar–OCH_3) integrated peak areas was 1:3, indicating that the aldehyde was retained during RAFT polymerization without protecting groups. Twenty mole percent of the aldehyde groups in **2a** ($M_{n,SEC}$ = 22,000 g/mol, $Đ$ = 1.30) were converted to dimethyl acetal groups upon washing with methanol. Reaction stoichiometry, methods, and additional molecular characteristics for each polymer are located in the Supporting Information (SI).

As expected for controlled RAFT polymerizations, the polymers had low dispersities that decreased with monomer conversion (Figure 1a and Figure S1, SI), and the syntheses

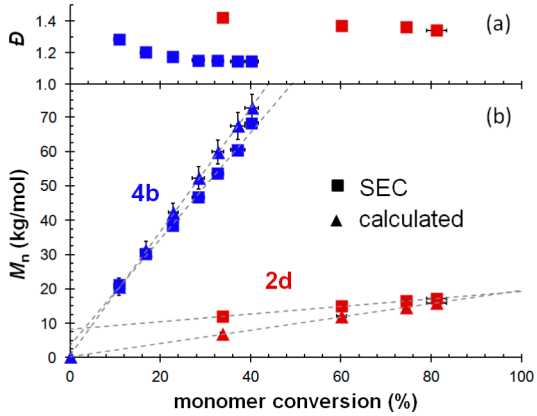

Figure 1. Relationship (a) between $Đ$ (as determined by SEC) and monomer conversion and (b) between M_n (as determined by SEC and calculated as described in the SI) and monomer conversion during the syntheses of **2d** (red in all figures) and **4b** (blue in all figures). Error bars represent 95% confidence intervals in ^{1}H NMR (vertical and horizontal) and stoichiometric (vertical) data. Linear regressions (dashed) guide the eye.

exhibited number-average molecular weights (M_n values) that increased linearly with monomer conversion (Figure 1b). Kinetic data also were obtained (Figure S2, SI) and suggest pseudo-first-order polymerization rates. The nonzero intercept of the linear regression for vanillin-based polymer **2d** (Figure 1b, SEC) likely indicates slow or incomplete consumption of the CTA as was the case for literature reports of cumyl dithiobenzoate–methyl methacrylate polymerizations that gave plots similar to Figure 1b and Figure S1 of the SI.[28] In contrast, the synthesis of fatty acid-based polymer **4b** ($M_{n,SEC}$ = 68,000 g/mol, $Đ$ = 1.14) demonstrated high initiation efficiency and consumption of the CTA, which is illustrated by the trendline that intersects the *y*-axis near the origin of Figure 1b (SEC). The small discrepancy in the $M_{n,SEC}$ and $M_{n,calculated}$ data from both syntheses also may be attributed to differences in hydrodynamic volume between the analyzed polymers and the PS standards used to estimate $M_{n,SEC}$.

Differential scanning calorimetry (DSC) data for polymers **2a**, **2d**, **4b**, and BCP **3b** are presented in Figure 2. As illustrated by transitions in these DSC data, the pure vanillin-based homopolymer and block (in the copolymer) had a T_g of 120 °C, and the fatty acid-based homopolymer and block had a melting temperature (T_m) of −33 °C. The T_g for **2a** was 111 °C, 9 °C lower than **2d**, presumably as a result of the free volume added by the dimethyl acetal groups. Transition measurements taken by Floudas et al. (T_m = −34 °C)[29] for poly(lauryl methacrylate) agree with data for **4b**, including the inability to resolve the polymer's T_g (−65 °C[20] or −48 °C[29]) from its overlapping melting transition by DSC. The two distinct transitions in the trace for **3b**, which match the

dx.doi.org/10.1021/sc400497a | ACS Sustainable Chem. Eng. 2014, 2, 569–573

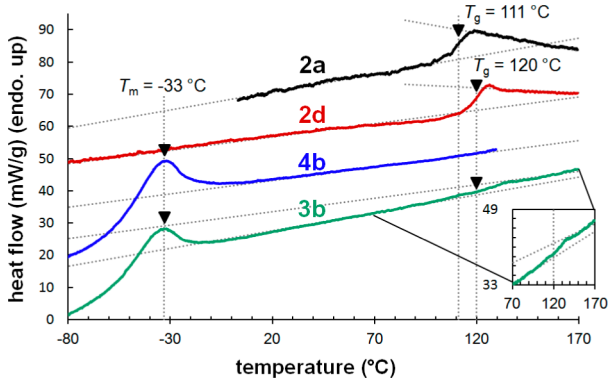

Figure 2. Second DSC trace on heating (2 °C/min, N_2 flow) for **2a** (black), **2d**, **4b**, and **3b** (green in all figures), normalized by mass and shifted vertically for comparison. Lines and arrows guide the eye to the T_g values (111 °C in **2a**, 120 °C in **2d** and **3b**) and T_m values (−33 °C in **4b** and **3b**).

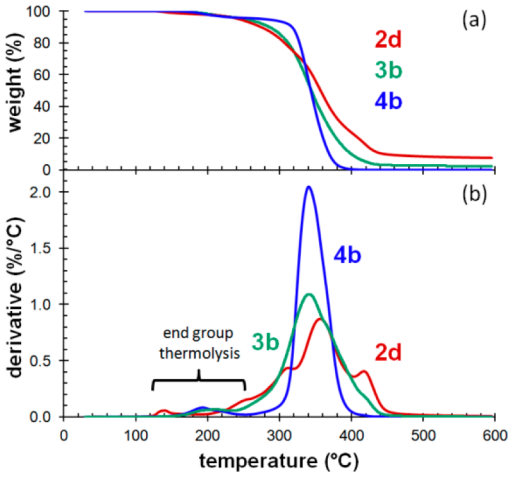

Figure 3. Representative TGA data (10 °C/min, N_2 flow) for **2**, **4**, and **3**. Normalized (a) sample weight percentage and (b) degradation rate (first-derivative) vs temperature on heating.

transitions from the homopolymers, suggest that nanoscale phase separation exists between blocks in the vanillin−fatty acid BCP.

DSC data for PS (200 kg/mol, $Đ \leq 1.05$) taken to compare against polymer **2d** gave a T_g of 104 °C, 16 °C lower than that of **2d**. With polymer **2a**, we were able to reduce the T_g of the vanillin-based polymer to within 7 °C of the PS's T_g by converting 20 mol % of the aldehydes to dimethyl acetal groups. The similarity between the T_g values for PS, **2d**, and **2a** supports the potential for implementing vanillin or other LMCs, such as guaiacol and creosol, as functionalized or nonfunctionalized PS-alternatives, respectively. On-demand polymers with T_g values of approximately 100 °C eventually may be prepared by selecting an appropriate combination of lignin monomers or level of dimethyl acetalization. As an example beyond dimethyl acetalization of vanillin, Stanzione et al. performed bulk free radical polymerizations on **1** and obtained a T_g of 98 ± 4 °C, 22 °C lower than **2d**, yet bulk free radical polymerizations of a different methacrylated LMC, methacrylated 4-propylguaiacol, gave a T_g of 73 ± 2 °C.[30] Conceivably, controlled (e.g., RAFT) polymerizations of methacrylated 4-propylguaiacol or other LMCs would produce polymers with T_g values even closer to 100 °C than **2d**'s T_g of 120 °C without the need for dimethyl acetalization.

Thermogravimetric analysis (TGA, 10 °C/min, N_2 flow) was performed on biobased polymers **2b**, **2d**, **4a** ($M_{n,SEC}$ = 77,000 g/mol, $Đ$ = 1.42), **4b**, and **3b** (data for **2b**, **4b**, and **3b** in Figure 3) to probe whether they are thermally stable for practical applications and processing. Additionally, PS (RAFT-PS, polymerized by RAFT with CTA = 2-cyano-2-propyl benzodithioate, $M_{n,SEC}$ = 24,400 g/mol, $Đ$ = 1.09) and PI (synthesized by anionic polymerization in 40 °C cyclohexane, 74% cis-1,4; 21% trans-1,4; 5% 3,4 or 1,2; $M_{n,SEC}$ = 540,000 g/mol; $Đ$ = 1.13) were examined by TGA (Figure S3, SI, also 10 °C/min under N_2 flow) to provide meaningful comparisons between biobased and petroleum-based polymers. In the first derivatives of the RAFT-synthesized polymers' mass-loss traces (Figure 3b), there are two distinct regions of accelerated degradation. The smaller peaks from ∼155−250 °C likely result from thermolysis of the benzodithioate ($C_7H_5S_2$) end groups. These peaks correspond to 1−5% mass loss (0.2−2% expected mass loss), depending on the polymer (and its molecular weight) and end group degradation mechanism. The end group thermolysis hypothesis is supported by detailed studies of RAFT-polymerized methacrylates and styrene performed by Moad and co-workers, in which comparable actual-versus-expected mass losses over similar temperature ranges (150−270 °C) were reported.[31,32] The largest peaks in Figure 3b representing degradation of the polymers' side groups and backbone have maxima (peak temperatures, T_p) at 356, 344, and 341 °C for **2d**, **4b**, and **3b**, respectively. Extrapolated onset degradation temperatures (T_o) taken at the intersection between the starting baseline and the tangent to the point of greatest slope in the mass-loss traces (Figure 3a) were 321 °C for **4b** and 300 °C for **2d** and **3b**. Comparing against the biobased polymers, measured T_p values for PS and PI (404 and 367 °C, respectively) were 11−63 °C higher, and measured T_o values for PS and PI (377 and 344 °C, respectively) were 23−77 °C higher. Note that the measured characteristic degradation temperatures for PS and PI in this work are 19−33 °C lower than reports with similar, albeit nonidentical, run conditions,[33,34] so the T_o and T_p values reported in this work likely underestimate each polymers' actual thermal stability.

The measured representative degradation temperatures, T_o and T_p, are well enough above each polymer's T_g such that they can survive typical processing temperatures of approximately 200−250 °C. Additionally, these vanillin- and fatty acid-based methacrylate polymers are at least as thermally stable as commercial biobased polyesters, such as polylactide (T_o ∼200−280 °C[35,36] depending on purity and heating rate).[37] However, high-temperature processing and usage of the vanillin-based polymers may be limited by their 11−77 °C lower degradation temperatures relative to similar petroleum-based polymers.

Small-angle X-ray scattering (SAXS) and transmission electron microscopy (TEM) data for BCP **3b** are presented in Figure 4 and illustrate its body-centered cubic (bcc) spherical morphology. Locations of the first minima and maxima for a form factor of spheres with an average radius of 12.5 ± 0.2 nm (dashed line in Figure 4a) match the minima and maxima in the 1-D SAXS profile. Further, the radius from the form factor is consistent with the average radius of 13.0 ± 0.3 nm predicted from the primary peak (q^* = 0.021 Å^{-1}) and a bcc-sphere geometry. The Bragg peaks at q/q^* = $2^{1/2}$, $4^{1/2}$, and $5^{1/2}$ denoted by arrows in Figure 4a support the bcc assignment. Minima in the spherical form factor, poor long-range order, and limitations in SAXS resolution presumably prevent additional

dx.doi.org/10.1021/sc400497a | ACS Sustainable Chem. Eng. 2014, 2, 569−573

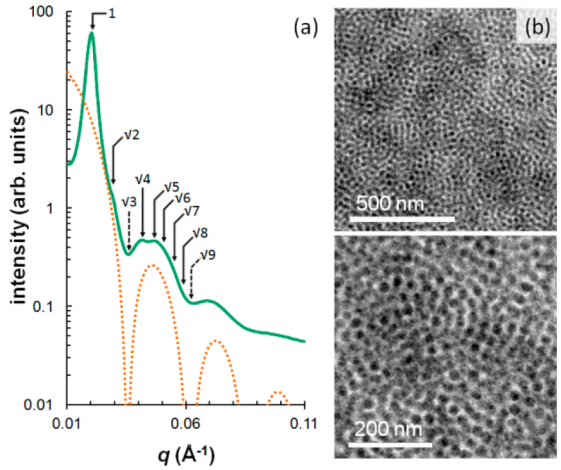

Figure 4. (a) 1-D SAXS data (solid) for BCP **3b** shifted vertically, plotted against scattering vector (q), and overlaid by a form factor for spheres with a radius of 12.5 nm (dashed). Arrows indicate Bragg peaks for bcc spheres, and dashed arrows mark peaks precluded by minima in the spherical form factor. (b) Representative TEM micrographs of **3b**, in which the dark spots correspond to RuO_4-stained vanillin-based polymer domains.

Bragg peaks expected for bcc spheres ($q/q^* = 3^{1/2}$ and any $n^{1/2}$, when n is any integer greater than or equal to 6) from being resolved. TEM micrographs of **3b** (Figure 4b) also support a spherical assignment, as the 2-D images display dark circles (**2d**-block with preferential affinity for the RuO_4 stain) inside a light matrix (fatty acid-block). The spheres have an average radius of 12 ± 1 nm, which is consistent with the SAXS data (13.0 ± 0.3 nm).

Together, these SAXS and TEM data (Figure 4) indicate that BCP **3b** self-assembles into vanillin-based spheres on a bcc lattice at 17 vol% **2d**-block. This morphological assignment is expected for amorphous bulk diblock copolymers of similar composition[38] and demonstrates the most common lattice packing for linear sphere-forming BCPs.[39] SAXS data for **3a** (20 vol % **2d**-block) also indicate existence of nanoscale phase separation; these data are located in Figure S4 of the SI.

CONCLUSIONS

Implications of these successful RAFT polymerizations and block copolymerizations of vanillin-based monomers primarily relate to the system's adaptability in affording on-demand properties to sustainable biobased homopolymers and BCPs. Foremost, LMCs, in addition to **1**, are expected to polymerize in a similar controlled fashion via the presented scheme. Analogous RAFT polymerizations with 2-cyano-2-propyl benzodithioate have been applied successfully to at least 10 other methacrylate monomers; none of which were potential lignin derivatives.[40] The properties afforded by the vanillin-based examples suggest the desirable characteristics likely exhibited by similar LMC systems, with T_g values near and above 100 °C and T_o values of at least 300 °C. Extension of the vanillin-based polymers with lauryl methacrylate yielded BCPs with self-assembled bcc-nanospheres. We expect to achieve other useful morphologies characteristic of BCPs, such as hexagonally packed cylinders and lamellae, at increasing volume fractions of the vanillin-based block. In the future, the full range of possible T_g values, T_o values, morphologies, and other relevant properties manifested by similar systems, including biodegradability, will be investigated as the library of lignin-based homopolymers and BCPs is expanded.

ASSOCIATED CONTENT

Supporting Information

Equipment, materials, methods, SEC traces, kinetic data, SAXS data for **3a**, and extended TGA data. This material is available free of charge via the Internet at http://pubs.acs.org.

AUTHOR INFORMATION

Corresponding Authors

*E-mail: wool@udel.edu (R.P.W.).
*E-mail: thepps@udel.edu (T.H.E.).

Present Address

[§]J.F.S.: Department of Chemical Engineering, Rowan University, Glassboro, New Jersey 08028, United States.

Author Contributions

[∥]A.L.H. and J.F.S. contributed equally to this work.

Notes

The authors declare no competing financial interest.

ACKNOWLEDGMENTS

The authors acknowledge a DuPont Young Professor Award to T.H.E. for the funding of A.L.H., the Strategic Environmental Research and Development Program (SERDP WP-1758) through the Cooperative Agreement W911NF-06-2-001 for the financial support of J.F.S. and R.P.W., the NSF CRIF: MU CEH 0840401 for supporting the University of Delaware NMR laboratory, and the W.M. Keck Electron Microscopy Facility for use of their TEM and ultramicrotome instruments. Use of the National Synchrotron Light Source (NSLS), Brookhaven National Laboratory, was supported by the U.S. Department of Energy, Office of Science, Office of Basic Energy Sciences, under Contract No. DE-AC02-98CH10886. We thank Dr. Lixia Rong for assistance with NSLS SAXS; Dr. Michael E. Mackay for use of his density kit, DSC, and TGA; Sarah Mastroianni for synthesizing PI; and Wei-Fan Kuan for synthesizing RAFT-PS.

REFERENCES

(1) Hadjichristidis, N.; Pispas, S.; Floudas, G. *Block Copolymers: Synthetic Strategies, Physical Properties, and Applications*; Wiley-Interscience: Hoboken, NJ, 2003.
(2) *Report on Carcinogens*, 12th ed.; U.S. Department of Health and Human Services, Public Health Service, National Toxicology Program: Research Triangle Park, NC, 2011.
(3) Mülhaupt, R. Green polymer chemistry and bio-based plastics: Dreams and reality. *Macromol. Chem. Phys.* **2013**, *214* (2), 159−174.
(4) Anastas, P.; Eghbali, N. Green chemistry: Principles and practice. *Chem. Soc. Rev.* **2010**, *39* (1), 301−312.
(5) Holmberg, A. L.; Stanzione, J. F., III; Wool, R. P.; Epps, T. H., III Bio-based block copolymer derived from lignin and plant oils. U.S. Provisional Patent Application 61/789,490, unpublished work, March 15, 2013.
(6) Gandini, A. The irruption of polymers from renewable resources on the scene of macromolecular science and technology. *Green Chem.* **2011**, *13* (5), 1061−1083.
(7) Jegers, H. E.; Klein, M. T. Primary and secondary lignin pyrolysis reaction pathways. *Ind. Eng. Chem. Process Des. Dev.* **1985**, *24* (1), 173−183.
(8) Brodin, I.; Sjöholm, E.; Gellerstedt, G. The behavior of kraft lignin during thermal treatment. *J. Anal. Appl. Pyrolysis* **2010**, *87* (1), 70−77.

(9) Mathers, R. T. How well can renewable resources mimic commodity monomers and polymers? *J. Polym. Sci., Part A: Polym. Chem.* **2012**, *50* (1), 1−15.
(10) Mosnáček, J.; Yoon, J. A.; Juhari, A.; Koynov, K.; Matyjaszewski, K. Synthesis, morphology and mechanical properties of linear triblock copolymers based on poly(α-methylene-γ-butyrolactone). *Polymer* **2009**, *50* (9), 2087−2094.
(11) Miyake, G. M.; Newton, S. E.; Mariott, W. R.; Chen, E. Y.-X. Coordination polymerization of renewable butyrolactone-based vinyl monomers by lanthanide and early metal catalysts. *Dalton Trans.* **2010**, *39* (29), 6710−6718.
(12) Wanamaker, C. L.; O'Leary, L. E.; Lynd, N. A.; Hillmyer, M. A.; Tolman, W. B. Renewable-resource thermoplastic elastomers based on polylactide and polymenthide. *Biomacromolecules* **2007**, *8* (11), 3634−3640.
(13) Robertson, M. L.; Hillmyer, M. A.; Mortamet, A.-C.; Ryan, A. J. Biorenewable multiphase polymers. *MRS Bull.* **2010**, *35* (3), 194−200.
(14) Mialon, L.; Vanderhenst, R.; Pemba, A. G.; Miller, S. A. Polyalkylenehydroxybenzoates (PAHBs): Biorenewable aromatic/aliphatic polyesters from lignin. *Macromol. Rapid Commun.* **2011**, *32* (17), 1386−1392.
(15) da Silva, E. A. B.; Zabkova, M.; Araújo, J. D.; Cateto, C. A.; Barreiro, M. F.; Belgacem, M. N.; Rodrigues, A. E. An integrated process to produce vanillin and lignin-based polyurethanes from Kraft lignin. *Chem. Eng. Res. Des.* **2009**, *87* (9), 1276−1292.
(16) Çayli, G.; Meier, M. A. R. Polymers from renewable resources: Bulk ATRP of fatty alcohol-derived methacrylates. *Eur. J. Lipid Sci. Technol.* **2008**, *110* (9), 853−859.
(17) La Scala, J. J.; Sands, J. M.; Orlicki, J. A.; Robinette, E. J.; Palmese, G. R. Fatty acid-based monomers as styrene replacements for liquid molding resins. *Polymer* **2004**, *45* (22), 7729−7737.
(18) Greenberg, S. A.; Alfrey, T. Side chain crystallization of *n*-alkyl polymethacrylates and polyacrylates. *J. Am. Chem. Soc.* **1954**, *76* (24), 6280−6285.
(19) Wang, X. A.; He, X. J.; Huang, G. S.; Wu, J. R. Correlations between alkyl side chain length and dynamic mechanical properties of poly(n-alkyl acrylates) and poly(n-alkyl methacrylates). *Polymer* **2012**, *53* (2), 665−672.
(20) Rogers, S. S.; Mandelkern, L. Glass transitions of the poly-(*n*-alkyl methacrylates). *J. Phys. Chem.* **1957**, *61* (7), 985−990.
(21) Cho, K. Y.; Hwang, S. S.; Yoon, H. G.; Baek, K.-Y. Electroactive methacrylate-based triblock copolymer elastomer for actuator application. *J. Polym. Sci., Part A: Polym. Chem.* **2013**, *51* (9), 1924−1932.
(22) Fielding, L. A.; Derry, M. J.; Ladmiral, V.; Rosselgong, J.; Rodrigues, A. M.; Ratcliffe, L. P. D.; Sugihara, S.; Armes, S. P. RAFT dispersion polymerization in non-polar solvents: Facile production of block copolymer spheres, worms and vesicles in *n*-alkanes. *Chem. Sci.* **2013**, *4* (5), 2081−2087.
(23) Chatterjee, D. P.; Mandal, B. M. Triblock thermoplastic elastomers with poly(lauryl methacrylate) as the center block and poly(methyl methacrylate) or poly(*tert*-butyl methacrylate) as end blocks. Morphology and thermomechanical properties. *Macromolecules* **2006**, *39* (26), 9192−9200.
(24) Chatterjee, D. P.; Mandal, B. M. The ATRP synthesis of the potential thermoplastic elastomer poly(methyl methacrylate)-b-(lauryl methacrylate)-b-(methyl methacrylate) hitherto unrealized by ionic polymerization. *Macromol. Symp.* **2006**, *240* (1), 224−231.
(25) Wang, S.; Kesava, S. V.; Gomez, E. D.; Robertson, M. L. Sustainable thermoplastic elastomers derived from fatty acids. *Macromolecules* **2013**, *46* (18), 7202−7212.
(26) Stanzione, J. F., III; Sadler, J. M.; La Scala, J. J.; Wool, R. P. Lignin model compounds as bio-based reactive diluents for liquid molding resins. *ChemSusChem* **2012**, *5* (7), 1291−1297.
(27) Semsarilar, M.; Perrier, S. 'Green' reversible addition-fragmentation chain-transfer (RAFT) polymerization. *Nat. Chem.* **2010**, *2* (10), 811−820.
(28) Han, X. Q.; Fan, J.; He, J. P.; Xu, J. T.; Fan, D. Q.; Yang, Y. L. Direct observation of the RAFT polymerization process by chromatography. *Macromolecules* **2007**, *40* (15), 5618−5624.
(29) Floudas, G.; Placke, P.; Štěpánek, P.; Brown, W.; Fytas, G.; Ngai, K. L. Dynamics of the "strong" polymer of *n*-lauryl methacrylate below and above the glass transition. *Macromolecules* **1995**, *28* (20), 6799−6807.
(30) Stanzione, J. F., III; Sadler, J. M.; La Scala, J. J.; Palmese, G. R.; Wool, R. P., The effect of methacrylated lignin model compound structure on the properties of high-performance polymers. In preparation, 2014.
(31) Postma, A.; Davis, T. P.; Moad, G.; O'Shea, M. S. Thermolysis of RAFT-synthesized polymers. A convenient method for trithiocarbonate group elimination. *Macromolecules* **2005**, *38* (13), 5371−5374.
(32) Chong, B.; Moad, G.; Rizzardo, E.; Skidmore, M.; Thang, S. H. Thermolysis of RAFT-synthesized poly(methyl methacrylate). *Aust. J. Chem.* **2006**, *59* (10), 755−762.
(33) Shapi, M. M. TG and DSC studies of some thermal properties and stability aspects of poly(acrylonitrile butadiene styrene), polystyrene and poly(acrylonitrile styrene) plastics. *Thermochim. Acta* **1991**, *175* (1), 25−34.
(34) Yao, Q.; Wilkie, C. A. How does cross-linking affect the thermal stability of polyisoprene? *Polym. Degrad. Stab.* **2000**, *69* (3), 287−296.
(35) Jamshidi, K.; Hyon, S.-H.; Ikada, Y. Thermal characterization of polylactides. *Polymer* **1988**, *29* (12), 2229−2234.
(36) Nalbandi, A. Kinetics of thermal degradation of polylactic acid under N_2 atmosphere. *Iran. Polym. J.* **2001**, *10* (6), 371−376.
(37) Carrasco, F.; Pagès, P.; Gámez-Pérez, J.; Santana, O. O.; Maspoch, M. L. Processing of poly(lactic acid): Characterization of chemical structure, thermal stability and mechanical properties. *Polym. Degrad. Stab.* **2010**, *95* (2), 116−125.
(38) Matsen, M. W. Effect of architecture on the phase behavior of AB-type block copolymer melts. *Macromolecules* **2012**, *45* (4), 2161−2165.
(39) Dormidontova, E. E.; Lodge, T. P. The order−disorder transition and the disordered micelle regime in sphere-forming block copolymer melts. *Macromolecules* **2001**, *34* (26), 9143−9155.
(40) Barner-Kowollik, C. *Handbook of RAFT Polymerization*. Wiley-VCH: Weinheim, Germany, 2008.